EasyChair Preprint

№ 9669

A Numerical Investigation on Improving the Hovering Efficiency of a UAV Helicopter with a Spherical Fuselage

Minh Trung Duong, Huy Cuong Do, Thi Kim Dung Hoang and Ich Long Ngo

February 5, 2023

A numerical investigation on improving the hovering efficiency of a UAV helicopter with a spherical fuselage

Minh Trung Duong[1], Huy Cuong Do[1], Thi Kim Dung Hoang[1], and Ich Long Ngo[1,*]
[1] *School of Mechanical Engineering, Hanoi University of Science and Technology, No. 01, Dai Co Viet, Hai Ba Trung, Hanoi, Vietnam*
*Email: long.ngoich@hust.edu.vn

Abstract. Traditional methods used for spraying a biochemical pesticide have been seriously affecting human health, the social system, and the natural eco-environment. Therefore, an UAV (Unmanned Aerial Vehicle) helicopter is considered as one of the most promising methods for reducing or preventing the negative impacts of pesticide spraying. The objective of the present study is to enhance the hovering efficiency of a UAV helicopter with a spherical fuselage under the effects of the fuselage size (R_f/R) and the distance between the fuselage and rotor (H_m/R), where R is the rotor radius. The RANS method combined with the k-ε turbulent model is used to model the airflow through the helicopter. The numerical model mentioned was well validated by comparing it with the results obtained in the literature. Consequently, the hovering efficiency which is frequently known as a figure of merit (FM), increases with either increasing R_f/R or decreasing H_m/R. A novel correlation which is as the function of R_f/R and H_m/R is first proposed for predicting the FM of UAV helicopters quickly and effectively. The results obtained in this study are very useful for enhancing the aerodynamic performance of UAV helicopters applied in various applications, particularly pesticide spraying in agriculture.

Keywords: Aerodynamic, Computational Fluid Dynamic, Helicopter, Turbulent flow, Unmanned Aerial Vehicle.

1. Introduction

Pesticide treatments are regarded as an important issue during plant protection activities in modern agriculture. Efficient application of pesticides may be useful to control plant pests and diseases to boost agricultural yields [1]. In Vietnam, the most common methods of spraying probiotics today are using a manual pesticide sprayer, a manual pesticide spraying machine, or a remote-control pesticide spraying machine. However, the traditional methods used for spraying probiotics have been seriously affecting human health due to close contact with the chemical, social system, and natural eco-environment but the effectiveness is low, the spray is uneven, depends on the terrain and the type of crop [2, 3]. To prevent human health issues with the manual spraying process, unmanned aerial vehicles (UAV) are considered as a promising candidate. In recent years, UAVs are commonly used in the field of precision agriculture in industrialized countries, and the UAV helicopter models are being developed for the relevant applications [1].

There have been some experimental studies of the impact of the number of blades on the profile drag of UAV helicopter rotors in hover [4] or model-based helicopter UAV control [5]. Therefore, studying the characteristics of helicopters to improve applicability and operation is receiving more and more attention and research. Nowadays, computational fluid dynamics (CFD) is a powerful tool that is used extensively in aerodynamic applications. It provides numerical solutions to fluid flow by solving governing equations, such as continuity, and Navier-Stokes equations. Using the CFD method, complicated problems can be simulated and analyzed. It has also been applied to study the aerodynamic phenomena through the helicopter's wings or the analysis of the aerodynamic interactions between the main rotor and the helicopter fuselage [6, 7]. Although the flight dynamic behaviors have been reported in previous studies for only the main rotor, to our best knowledge, no research considers the effects of the fuselage on the aerodynamic performance of a UAV helicopter in a hovering regime. Particularly,

no research provides a generalized correlation for predicting the hovering efficiency of UAV helicopters quickly and effectively.

The objective of the present study is to improve the hovering efficiency of a UAV helicopter with a spherical fuselage. The RANS method combined with the *k-ε* turbulent model was used to simulate the fluid flow through the main rotor and the fuselage. The flow behaviors were found under the effects of two main parameters, the distance between the rotor and the fuselage and the fuselage size. Additionally, the fitting method was utilized to find out the correlation between FM and these two parameters.

2. Numerical methodology

2.1. Numerical model

The Navier-Stokes equations are the fundamental governing equations for describing the behaviors of a fluid flow. It is obtained by applying Newton's Law of Motion to a fluid particle and is called the momentum equation. Additionally, the mass conservation equation is known as the continuity equation. These equations are shown in Eqs. (1-2)

$$\frac{\partial \rho}{\partial t} + \frac{\partial}{\partial x_i}(\rho u_i) = 0 \tag{1}$$

$$\frac{\partial \rho u_i}{\partial t} + \frac{\partial}{\partial x_j}(\rho u_i u_j) = -\frac{\partial p}{\partial x_i} + \frac{\partial}{\partial x_j}\left[\mu_{eff}\left(\frac{\partial u_i}{\partial x_j} + \frac{\partial u_j}{\partial x_i}\right)\right] \tag{2}$$

where u_i, u_j are the velocity component in the corresponding direction, respectively. p, ρ, and μ_{eff} are the pressure, density, and dynamic viscosity of the fluid, respectively.

The *k-ε* turbulence model used is used. It is the most common model used in computational fluid dynamics (CFD) to simulate mean flow characteristics for turbulent flow conditions. It is a two-equation model that gives a general description of turbulence using two transport equations. The originality of the *k-ε* model was to either improve the mixing-length model or find an alternative to algebraically prescribing turbulent length scales in moderate to high complexity flows [1].

$$\frac{\partial(\rho k)}{\partial t} + \frac{\partial(\rho k u_i)}{\partial x_i} = \frac{\partial}{\partial x_j}\left[\frac{\mu_t}{\sigma_k}\frac{\partial k}{\partial x_j}\right] + 2\mu_t E_{ij} E_{ij} - \rho\varepsilon \tag{3}$$

$$\frac{\partial(\rho \varepsilon)}{\partial t} + \frac{\partial(\rho \varepsilon u_i)}{\partial x_i} = \frac{\partial}{\partial x_j}\left[\frac{\mu_t}{\sigma_\varepsilon}\frac{\partial \varepsilon}{\partial x_j}\right] + C_{1\varepsilon}\frac{\varepsilon}{k}2\mu_t E_{ij} E_{ij} - C_{2\varepsilon}\rho\frac{\varepsilon^2}{k} \tag{4}$$

where E_{ij} is a component of the rate of deformation. μ_t is eddy viscosity that is defined as:

$$\mu_t = \rho C_\mu \frac{k^2}{\varepsilon} \tag{5}$$

In the Eqs. (3-4) above, σ_k, σ_ε, $C_{1\varepsilon}$, $C_{2\varepsilon}$, and C_μ are semi-empirical coefficients. The values of these coefficients were found by numerous iterations of data fitting for a wide range of turbulent flows. These are given by: C_μ=0.09, σ_k=1.00, σ_ε=1.30, $C_{1\varepsilon}$=1.44, $C_{2\varepsilon}$=1.92.

The symmetric airfoil of the NACA0015 section was used with the chord length, c, of 0.13 m, radius, R, of 1.6 m, and angle of attack, α of 8°. The rotor is assumed to be a rigid body and blade flapping dynamics and tail rotor were neglected for simplicity. The fluid domain surrounding the rotor is cylindrical with a radius, height above the rotor and height below the rotor being 5R, 2.5R, and 5R, respectively, as shown in Fig. 1. The tetrahedron mesh was used for the blocks involved the rotor and fuselage, otherwise, the hexahedron mesh was used for the remaining blocks.

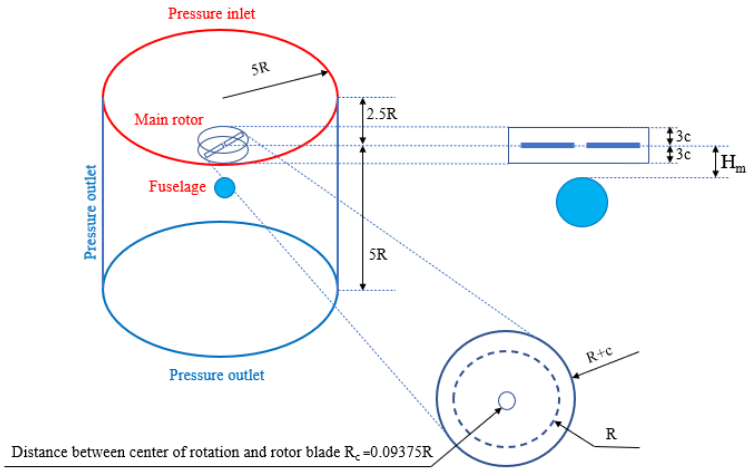

Figure 1. Schematic of the numerical model and boundary conditions.

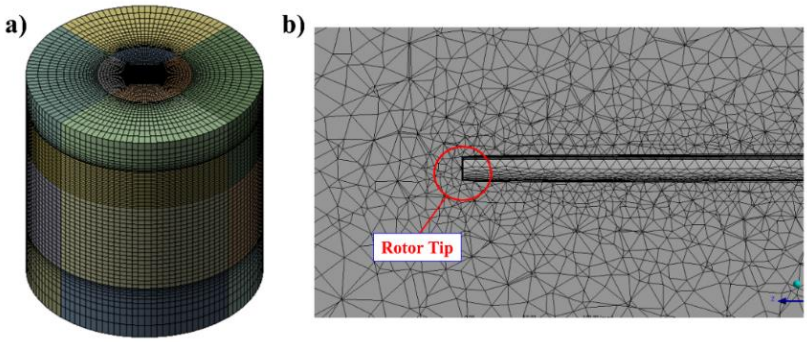

Figure 2. Overall mesh and streamwise section

Table 1. Mesh convergence test, Re_{tip} = 791,221, σ = 0.052

Grid model	No. of cells (×10^6)	*T* (N)	Relative error (%)
#1	2.23	344.86	2.53
#2	2.26	353.82	1.40
#3	**2.28**	**358.83**	**0.72**
#4	2.34	361.42	0.16
#5	2.36	361.99	

An important parameter to characterize the boundary layer problem near the solid wall in the turbulence flow is y^+. It varies from 17 to 60. Additionally, H_m is the distance between the main rotor and the fuselage of the helicopter. Based on the simulation, the thrust of the rotor T and the torque Q can be obtained. The coefficients of the thrust and power C_T and C_P are defined by Eq. (6) below.

$$C_T = \frac{T}{\rho A \Omega^2 R^2};\ C_P = \frac{Q}{\rho A \Omega^2 R^3} \tag{6}$$

Particularly, the figure of merit (*FM*) is defined by Eq. (7). The hovering efficiency of helicopter rotors is characterized by this non-dimensional parameter, which provides a common base for comparison between rotors with different geometries.

$$FM = \frac{C_T^{3/2}}{\sqrt{2}C_P} \tag{7}$$

The mesh convergence test was also carried out in the present study, as shown in Table 1. Five grid models from model #1 to model #5 were used with a number of cells ranging from 2.23×10^6 to 2.36×10^6. Notably, the Reynolds number of 791,221 and the solidity of 0.052 were used here. It was found that the result of rotor thrust is converged when the grid model is refined in this range. The relative error between the thrust from the coarse grid model and that of the finer grid model reduces to a small value. Based on these results, grid model #3 was used for further computations in the present study.

2.2. Code validation

The numerical model mentioned in Section 2.1 was first validated quantitatively by comparing the present results with both the experimental and numerical data obtained by Robinson et al. [7], as shown in Fig. 3. In this figure, a thrust ratio (T/T') is as a function of a distance between the rotor and the ground (H_g). Notably, T' denotes the baseline thrust that the main rotor is so far enough that the ground effect can be neglected. It was found that H_g/R is greater than 5. Consequently, Fig. 3 indicates that the numerical results are in very good agreement with the results obtained by Robinson et al. [7]. At this point, the thrust ratio decreases with increasing distance between the rotor and the ground. The maximum deviation is less than 3% compared with the experimental results. Furthermore, the present results are shown in Fig. 3 to predict more accurately than even the numerical results obtained by Robinson et al. [7] at high H_g/R. Therefore, this numerical model is well validated, and it can be used for studying qualitative flow behavior through the main rotor of a UAV helicopter.

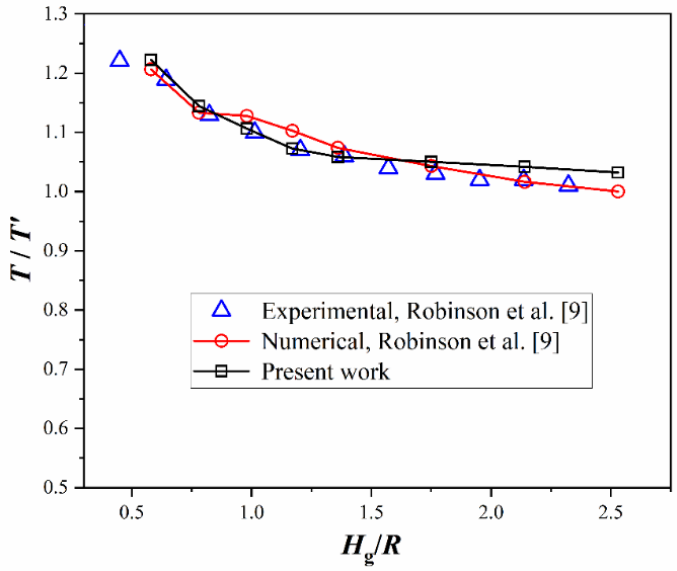

Figure 3. Comparing the present results with those obtained by Robinson et al. [7], Re = 32400, σ = 0.1, 2 blades with NACA0009.

3. Results and discussions

Fig. 4 shows the flow field surrounding the main rotor at Re = 791221, σ = 0.052. It was found from Fig. 4(a) that the air flow moves down in a vertical direction. This is essential due to the lifting effect acting on the rotor blades when they rotate at a specific speed. Additionally, it was observed that the region of very low pressure appears near the rotor tip on the suction surface, as shown in Fig. 4(b). Vacuum pressure is available in this region. As a result, the vortex tip can form naturally, and an induced drag may increase, hence the hovering efficiency reduces significantly. Therefore, the appropriate methods should be considered to prevent and confine this phenomenon.

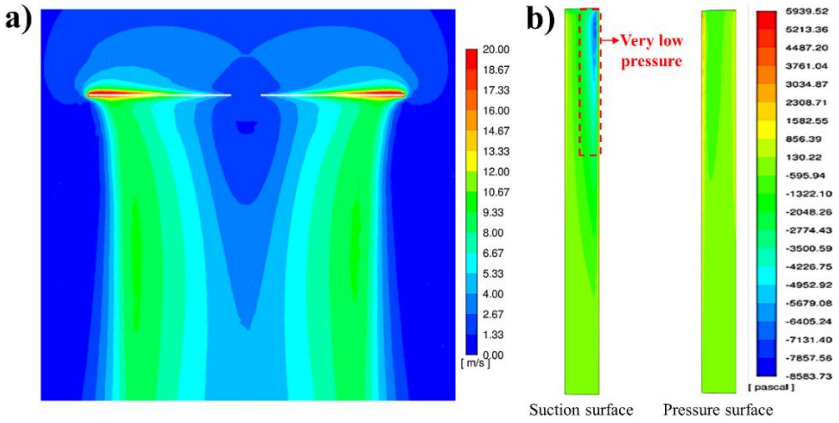

Figure 4. Flow field surrounding the main rotor, (a) Velocity contour on plane x = 0.0, and (b) pressure contour on the blade surfaces. Re = 791221, NACA0015, and σ = 0.052 were used.

To observe more obviously the variation of pressure along the rotor blade, pressure contours on some cross-sections are shown in Fig. 5. Four cross-sections were defined by *z*/*R* of 0.45, 0.60, 0.75, and 0.90. It was found from Fig. 5 that the region of low pressure mainly appears on the suction surface, and it expands from the rotor hub to the region near the rotor tip. This is due to the fact that the peripheral velocity increases functionally from the rotor hub to the rotor tip, the separation flow frequently appears at high-speed flow with the same angle of attack used, this results in the region of low pressure on the suction surface of the main rotor. In addition, this phenomenon also depends on the swirling flow formed in the region between two blades and the downstream flow, as shown in Fig. 6. The total induced drag from these regions plays an important role in determining the hovering efficiency of the UAV helicopter.

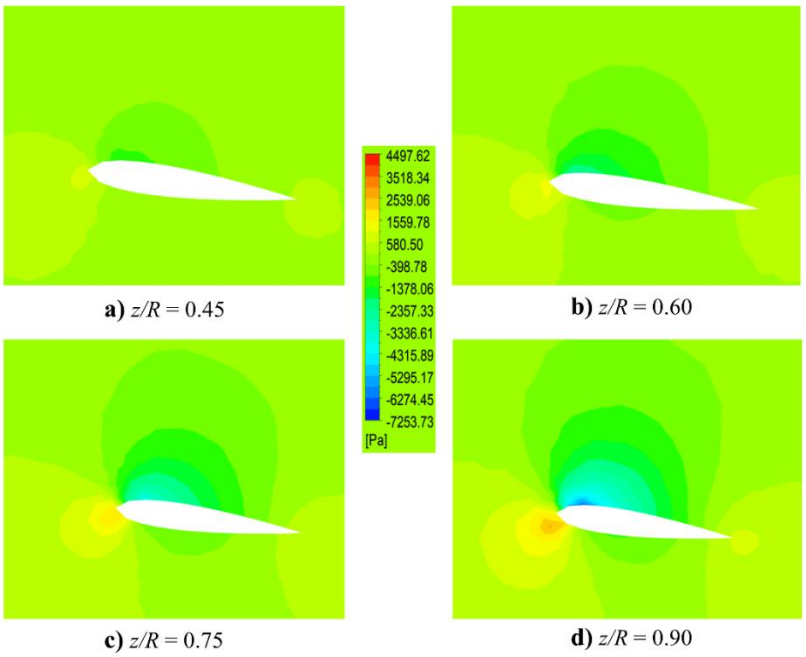

Figure 5. Pressure contour on some cross-sections perpendicular to a rotor blade.

The effect of the spherical fuselage on the flow behaviors of the airflow through the main rotor is shown in Fig. 7. H_m/R=0.5 and R_f/R=0.5 are used as a particular operating condition. Fig. 7 indicated that the flow behavior through the main rotor is affected significantly by the fuselage. This makes more sense as indicated by the results in Fig. 8 when the fuselage size increases. This is because the presence of the fuselage changes the swirling flow mentioned in Fig. 6, and finally, the total induced drag in the

whole helicopter is influenced. It implies that the hovering efficiency of the UAV helicopter can be improved using an appropriate size of the fuselage.

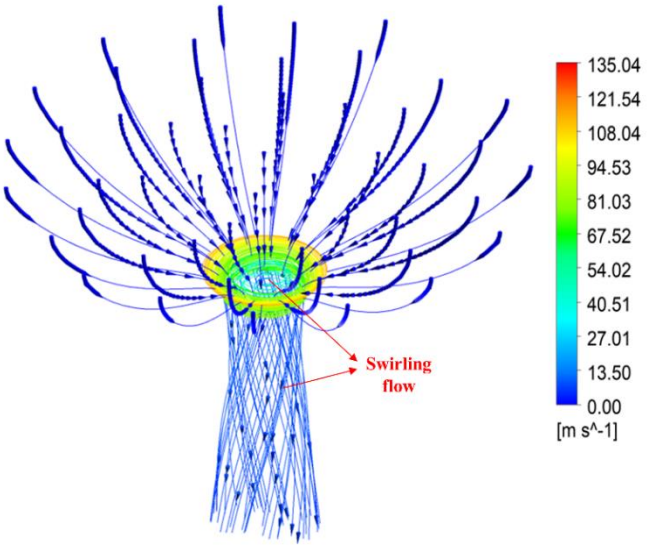

Figure 6. Swirl flow through main rotor.

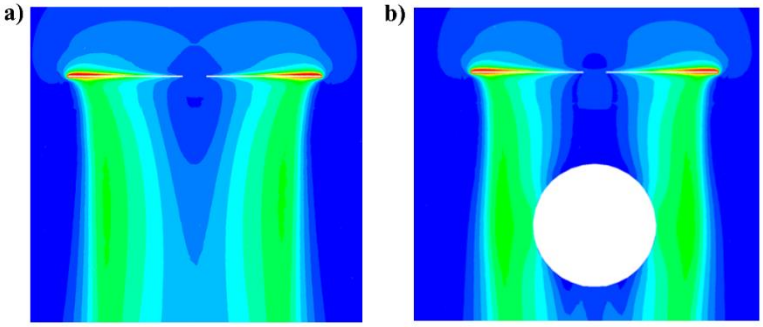

Figure 7. Velocity contour on plane x = 0.0, (a) without and (b) with fuselage, H_m/R=0.5, R_f/R=0.5

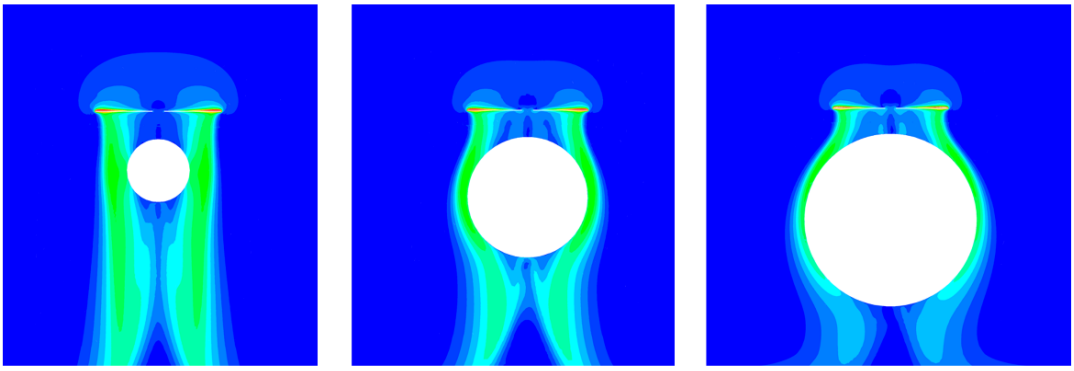

a) $R_f/R = 0.5$ **b)** $R_f/R = 1.0$ **c)** $R_f/R = 1.5$

Figure 8. Effects of the fuselage size, (a) R_f/R = 0.5, (b) R_f/R = 1.0, and (c) R_f/R = 1.5, H_m/R = 0.44 were used for all cases.

The effect of the distance between the rotor and the fuselage is also considered in this study, as shown in Fig. 9. This distance is specified at H_m/R = 0.29, 0.74, and 3.24 while keeping the fuselage

size at R_f/R = 1. It revealed that the downstream flow also depends on the distance between the rotor and the fuselage, particularly at low values H_m/R of 0.29 (Fig. 9(a)) and 0.74 (Fig. 9(b)). On the other hand, this influence gradually becomes smaller when the fuselage moves far from the main rotor, as shown in Fig. 9(c). It is predicted that the hovering efficiency decreases with increasing H_m/R.

To qualitatively examine the effects of the fuselage on the hovering efficiency of the UAV helicopter, the figure of merit was calculated for the large range of H_m/R. Three particular cases of R_f/R, i.e., less than (0.5), equal to (1.0), and greater than (1.5) the rotor radius, were used. The results obtained are shown in Fig. 10. It was found from this figure that *FM* increases with either decreasing the distance between the rotor and the fuselage or increasing the fuselage size. Additionally, it approaches a plateau value when H_m/R increases up to the high value or even the infinity.

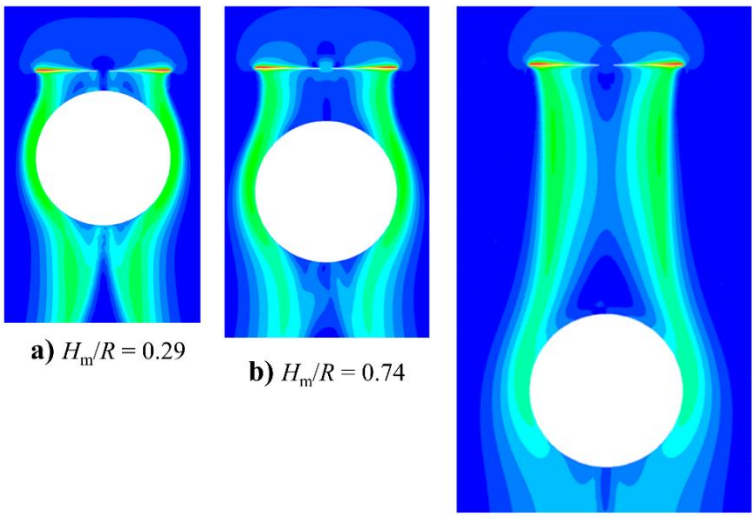

Figure 9. Effects of the distance between the rotor and the fuselage, (a) H_m/R = 0.29, (a) H_m/R = 0.74, and (a) H_m/R = 3.24, R_f/R = 1 was used for all cases.

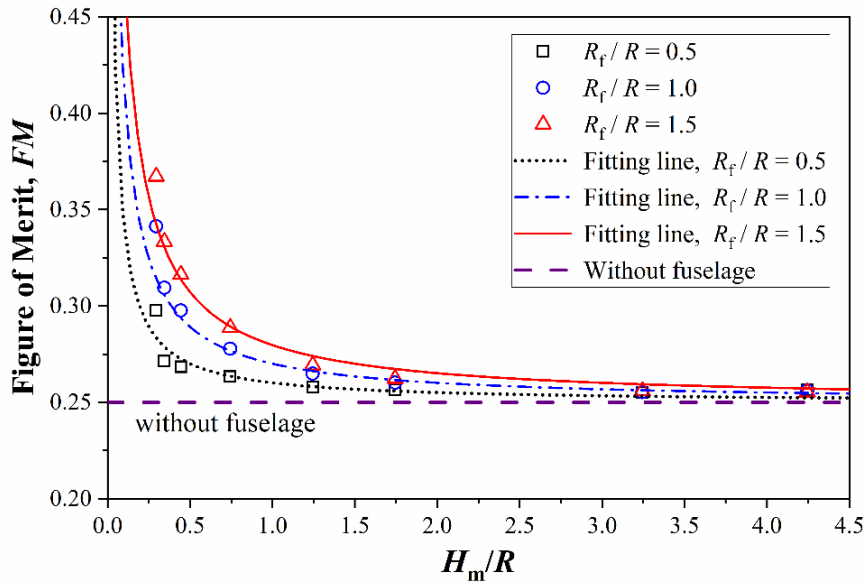

Figure 10. FM results in various models

Based on the computational data, a new correlation is proposed using the fitting method, as shown in Eq. (8). The results from this correlation are also represented in Fig. 10 by the fitting lines. The

maximum deviation is less than 8% for the whole considered range of H_m. In a physical viewpoint, this correlation satisfies an important aspect as follows: *FM* approaches a constant value (i.e., 1/4 or 0.25) when H_m goes to infinity or R_f equals zero. In this regard, the influence of the fuselage presence can be neglected, or no fuselage is used in the helicopter, as shown by the dash horizontal line in Fig. 10. In summary, this correlation is very useful in effectively predicting the *FM* of the UAV helicopter.

$$FM = \frac{H_m + 0.11R_f}{4H_m + 0.11R_f} \tag{8}$$

4. Conclusion

The aerodynamic behavior of the airflow through a UAV helicopter with a spherical fuselage has been examined in the hovering regime. The effects of the fuselage size (R_f/R) and the distance between the fuselage and the rotor (H_m/R) are carried out by the numerical approach. The RANS method combined with the *k-ε* turbulent model is used to model the airflow through the helicopter. Consequently, the flow behavior through the main rotor is affected significantly by the presence of the fuselage. *FM* increases with either decreasing the distance between the rotor and the fuselage or increasing the fuselage size. It means that the hovering efficiency of a UAV helicopter can be enhanced using a fuselage with an appropriate size and distance to the main rotor. Particularly, the novel correlation between *FM* and the two aforementioned parameters by Eq. (8) is first proposed for predicting the *FM* quickly and effectively. In summary, the results obtained in this study are very useful for enhancing the aerodynamic performance of UAV helicopters applied in various applications, particularly pesticide spraying in agriculture. The benchmark and optimization studies will be carried out for R_f/R and H_m/R parameters to maximize the hovering efficiency.

Acknowledgments

This research is funded by the Hanoi University of Science and Technology (HUST) under project number T2022-PC-017. We also express thanks to members in Truth Love in Simulation Laboratory (TLS Lab) and the Computer Aided Engineering Laboratory (CAE Lab) for their valuable support.

References

[1] A. Hafeez, M. A. Husain, S. P. Singh, A. Chauhan, M. T. Khan, N. Kumar, A. Chauhan, S. K. Soni, Implementation of drone technology for farm monitoring & pesticide spraying: A review, *Information Processing in Agriculture,* (2022), pp. 1-12.

[2] H. Berg, N. T. Tam, Use of pesticides and attitude to pest management strategies among rice and rice-fish farmers intheMekong Delta, Vietnam, *International Journal of Pest Management,* **58**, (2), (2012), pp. 153-164.

[3] V. N. Huyen, N. Van Song, N. T. Thuy, L. T. P. Dung, L. K. Hoan, Effects of pesticides on farmers' health in Tu Ky district, Hai Duong province, Vietnam, *Sustainable Futures,* **2**, (2020), pp. 1-12.

[4] F. Panayotov, I. Dobrev, F. Massouh, M. Todorov, Experimental study of the impact of the number of blades on the profile drag of UAV helicopter rotors in hover, *IOP Conference Series: Materials Science and Engineering*, *IOP Publishing*, (2020), pp. 1-8.

[5] B. Godbolt, A. F. Lynch, Model-based helicopter UAV control: experimental results, *Journal of Intelligent & Robotic Systems,* **73**, (1), (2014), pp. 19-31.

[6] T. D. Pham, A. T. Nguyen, N. T. Dang, V. U. Pham, On the aerodynamic interactions analysis between the main rotor and the helicopter fuselage, *Kalpa Publications in Engineering,* **3**, (2020), pp. 123-132.

[7] D. C. Robinson, H. Chung, K. Ryan, Numerical investigation of a hovering micro rotor in close proximity to a ceiling plane, *Journal of Fluids and Structures,* **66**, (2016), pp. 229-253.